ELSEVIER

Progress in Organic Coatings 56 (2006) 135–145

PROGRESS IN ORGANIC COATINGS

www.elsevier.com/locate/porgcoat

Incorporation of benzoic acid and sodium benzoate into silicone coatings and subsequent leaching of the compound from the incorporated coatings

Abdulhadi A. Al-Juhni, Bi-min Zhang Newby *

Department of Chemical and Biomolecular Engineering, The University of Akron, Akron, OH 44325-3906, United States

Received 16 June 2005; received in revised form 20 January 2006; accepted 24 February 2006

Abstract

Benzoic acid and sodium benzoate, two less toxic antifoulants as compared to currently used biocides in marine biofouling protection, were incorporated into silicone coatings to investigate their release behaviors and antifouling capabilities. It was found that benzoic acid, although exhibiting excellent antifouling capability, formed large crystals inside the coating regardless of the solvent used to increase its miscibility with silicone. The large crystals were found to be responsible for the fast leaching of the compound from the carrier coating, thus eliminating the long-term usefulness of the coating. Sodium benzoate, which was highly immiscible with silicone, was able to be incorporated into silicone in the form of small aggregates, and by tuning the preparation conditions, the aggregate size (hence the number of aggregates) could be varied. Leaching of sodium benzoate from silicone was determined to be much slower than that of benzoic acid, and a direct relationship between the leaching rate and the number of aggregates was observed. The sodium benzoate incorporated coating was found to exhibit enhanced antibacterial performance, and, for coatings containing 1 wt.% of sodium benzoate, a ∼50% reduction in bacterial attachment was achieved.

Keywords: Antifoulant; Benzoic acid; Sodium benzoate; Silicone coatings; Antifoulant leaching; Bulk entrapment

1. Introduction

Marine biofouling is the accumulation and growth of marine organisms on surfaces of structures immersed in natural water [1,2]. Biofouling causes serious problems to the marine industry [3]. The layer of attached organisms on ship's hulls decreases ship's speed and increases fuel consumption. As an example, the US Navy estimates that biofouling costs over US$ 150 million annually in excess fuel consumption and cleaning for naval vessels. Biofouling is also directly responsible for the bio-corrosion and other related problems [4–7].

Antifouling paints have long been the most effective method to prevent biofouling, where biocides or heavy metal compounds such as tributyltin (TBT) oxide are released from the coatings and inhibit microorganism's attachment. TBT compounds were found to be the most effective for biofouling prevention. Unfortunately, they are also the most toxic compounds against non-target marine organisms [8,9]. As a result, the International Maritime Organization (IMO) has banned the application of TBT compounds on January 1 of 2003, and the entire removal of TBT coatings by year 2008 will be required worldwide [10]. Therefore, considerable efforts are currently being committed to search for non-toxic or less toxic antifouling alternatives, including the assessment and usage of various pesticides, insecticides, and food preservatives such as benzoic acid.

Benzoic acid and its sodium salt (sodium benzoate) are the most common, safe, food preservatives and antimicrobial agents. Benzoic acid and sodium benzoate are classified in the United States as Generally Recognized as Safe (GRAS) and their use in food is permitted up to the maximum level of 0.1% [11]. From Microtox studies, the toxicity, in terms of the concentration that eliminates 50% of bacterial population or EC_{50}, of benzoic acid and sodium benzoate was determined to be ∼7 and ∼560 mg/l [12], respectively, which were three to five orders of magnitude lower than that of TBT (∼0.01–0.02 mg/l). Recognizing also the commercial availability and low cost of benzoic acid and sodium benzoate, they are attractive candidates to be incorporated into coatings as environmentally benign alternatives.

* Corresponding author. Tel.: +1 330 972 2510; fax: +1 330 972 5856.
E-mail address: bimin@uakron.edu (B.-m.Z. Newby).

0300-9440/$ – see front matter © 2006 Elsevier B.V. All rights reserved.
doi:10.1016/j.porgcoat.2006.02.009

In general, two antifouling mechanisms are suggested for the effectiveness of the non-toxic compounds: repellency and chemical anti-adhesive [13,14]. As emphasized by Railkin [14], the following exact definition should be applied to assign the non-toxic repellency mechanism for a certain antifouling compound: "Repellents are cues inducing a negative motor response, taxis, or kinesis in organisms at a certain stage of development, which causes them to move away from the source of these cues" [14]. This precise definition differentiates the true repellent property (a non-toxic mode of action) from other toxic properties of the antifouling material. For this definition to be applied, special experimental behavioral tests should be performed. However, in most studies, the true repellent function of various natural and synthetic antifoulants was hypothetically assumed rather than experimentally verified [14]. Among a few studies that followed the standard behavioral tests, benzoic acid was proven to have a true repellent mechanism as a non-toxic mode of action [14]. In addition to the repellency mechanism, the non-toxic antifouling compounds could also exhibit the chemical anti-adhesive mechanism, where molecules of the antifouling compound exist freely in water and act as catalytic inhibitors for the biochemical reactions involved in cell adhesion. The word "chemical" is used to distinguish this mechanism from the physical anti-adhesive mechanism, which usually is referred to as the easy-release silicone coatings. Following two controlled experimental test procedures that exist in the literature to verify the chemical anti-adhesive mechanism, benzoic acid was also proven to have chemical anti-adhesive properties [14]. Previous works for evaluating the antibacterial behaviors of benzoic acid have concluded that, at different points of the citric acid cycle, benzoic acid deactivates the enzymes that control acetic acid metabolism and oxidative phosphorilation in yeast and bacteria [15]. In a recent review on antibacterial mechanisms [16], benzoic acid was believed to act by interfering with the ability of the cell membrane to maintain a suitable pH level, which consequently lead to acidification of the cell interior and widespread disruption of the metabolism process [17]. Thus, benzoic acid appears to exhibit both non-toxic modes of actions (repellency and chemical anti-adhesive), highlighting the possibility of it being effective against broad spectra of micro and macro fouling species. In addition, field studies have shown that benzoic acid, when added to a vinyl-rosin coating, was effective in inhibiting different species of both micro and macro foulers [14], making it a very attractive non-toxic or less toxic antifouling candidate. However, due to the extremely fast leaching of the compound, the effectiveness of the coating with benzoic acid incorporated was only for a short period of time (1 month). Therefore, for further utilization of benzoic acid, understanding the cause for its fast leaching is essential and seeking techniques to incorporate benzoic acid into a coating to control its leaching is also important.

The salt form of benzoic acid, such as sodium benzoate (NaB) is even more environmentally benign as compared to benzoic acid. Static biological assays have also shown that NaB showed a narcotic (non-toxic) effect on the investigated microorganisms [18]. In addition to sodium benzoate, other different benzoic acid salts (calcium benzoate and aluminum benzoate) have also been tested by biological assays, and antifouling effectiveness similar to NaB were observed [18]. The mode of action for sodium benzoate was not precisely identified as for the case of benzoic acid, but the above study may indicate that the benzoate anion freely floating in water is important to the antifouling capabilities of NaB, and that the antifouling mechanism of NaB might be similar in some aspects as that of benzoic acid [18,19]. Nevertheless, field studies have shown that sodium benzoate when incorporated into a marine paint was successful for inhibiting marine microorganism attachments [19].

Both benzoic acid and sodium benzoate could be incorporated into foul-release coatings to achieve a synergistic effect wherein the antifouling properties of benzoic acid or NaB can be combined with the foul-release performance of the coating. Attributing to its low surface energy and extremely low elastic modulus, silicones have been considered one of the most attractive foul-release marine coatings [20–25]. In this project, two types of silicones: a transparent model coating, Sylgard® 184, and a commercial coating RTV11 were utilized as the coating carriers. The focus of this project was to first examine the reasons behind the fast leaching of benzoic acid when entrapped inside a coating, then to experimentally obtain benzoic acid or sodium benzoate incorporated silicone coatings with minimum alterations in surface and bulk properties of the coatings while attaining an adequate leaching rate such that the incorporated coatings were capable of preventing bacterial attachment for a long period of time.

2. Experimental

2.1. Materials

RTV11 and Sylgard® 184 were purchased from GE and Dow Corning, respectively. RTV11 came from the manufacturer in two parts: a polymer base (a hydroxy-terminated PDMS) and a catalyst (dibutyltin dilaurate or DBT). Included in the polymer base are the cross-linking agent (ethyl silicate 40) and the filler (calcium carbonate). Sylgard® 184 also came in two parts: a polymer base containing vinyl-terminated-PDMS and a curing agent having SiH-terminated-PDMS and the Pt-catalyst. Benzoic acid (99% pure) and NaB (99% pure, in powder form) were purchased from Sigma and Aldrich Chemical Inc. and used as received. Toluene, acetone, acetonitrile, and ether (ACS reagent, 99.5% pure) were purchased from VWR and also used as received. Microscopic glass slides (pre-cleaned, size: 25 mm × 75 mm × 1 mm) were obtained from VWR and used as received.

2.2. Coatings preparation and processing

Aware that the roughness of coating could have considerable effects on bacterial attachment, benzoic acid (BA) and sodium benzoate (NaB) were first homogenized with the base polymer using a suitable solvent, and then the mixture was blended with the catalyst to obtain a relatively smooth and uniform coating. Since benzoic acid has a relatively high solubility (10–30 wt.%) in most organic solvents (four of them used in this study were

toluene, acetone, ether, and acetonitrile) that are miscible with silicone, benzoic acid was dissolved in the organic solvent before addition to the silicone and then the solution was homogenized with the silicone base at a mass ratio of 20:80 solvent:polymer with rigorous mixing. NaB, on the other hand, is much more inorganic in nature, and has low solubility in organic solvents. It was first dissolved in de-ionized water, and then a water-miscible organic solvent, such as acetone, was added to the aqueous phase in different ratios while maintaining the complete solubility of NaB in the mixed-solvent. Acetone was used in our study, because it is also highly miscible with silicone, and has a high volatility. The BA or NaB solution, with the proper concentration, was homogenized with the silicone base with rigorous mixing. The mixtures were left inside the fume-hood at ambient conditions for 2 days, and then placed under vacuum at room temperature for 20 min, to remove the solvent. After that, the DBT catalyst (for RTV11 case) or the curing agent (for Sylgard® 184 case) was added according to the manufacturer's prescribed ratio (0.5 wt.% of DBT/RTV11, and 1:10 mass ratio for Sylgard® 184). Finally, each mixture (∼6.0 g) was poured into a polystyrene Petri dish with a diameter of 9 cm, and left to cure at ambient conditions for 1 week. This produces a film thickness of about 900 μm. For producing thinner films, the above mixtures (∼0.3 g) were spread out on glass substrates (surface area of about 1.2 cm × 5 cm) by means of the Doctor-Blade method, which resulted in film thickness of about 500 μm.

2.3. Coatings characterization

Variations in the morphology of benzoic acid and NaB incorporated silicone films were observed using an optical microscope (Model IX-70, Olympus) having video and still image capturing capabilities. Coating surface wettability was evaluated using the contact angle goniometer video system with de-ionized water as the probe liquid. Both dynamic and static contact angles were measured via the sessile drop method. For dynamic angles, the advancing and receding angles were achieved by the addition and removal, respectively, of water from the drops formed on the coating surface. For static angles, the water drop was placed on the coating surface and let to equilibrate without external force. Images of the drops were captured using the Dazzle Digital Video Creator (DVC) and its software, and data were processed using the Scion Image Software.

Elastic modulus of the coating was measured to evaluate the variation in bulk coating properties. Elastic modulus measurements for benzoic acid and NaB-blended RTV11 coatings, due to their opaque nature, were conducted using the stress–strain method. In that, a small rectangular sheet (length ∼25 mm, width ∼6 mm, and thickness ∼1 mm) of coating was vertically hung in air, its elongation under a particular weight was measured from the magnified images captured using the goniometer video system and the Dazzle DVC and its software. Stress [weight/(width × thickness)] was varied gradually up to ∼0.13 MPa. For BA and NaB-blended-Sylgard® 184 coatings, which were transparent, their bulk modulus were measured by the contact mechanics (JKR: Johnson–Kendall–Roberts [26]) method. The modulus of Sylgard® 184 based coatings could also be measured via the stress–strain technique, we chose the JKR technique because of the extensive usage of the JKR technique for evaluating the properties of Sylgard® 184 [27], and the values measured in this study could be compared to the reported values. In contact mechanics, a soft elastic lens is brought into contact with an elastic surface, and the deformation of the contact zone (normally a circular area) under a certain load can be related to the elastic modulus of the system, thus the modulus of the coating. The detailed theory behind the JKR technique can be found elsewhere [26,27]. For the JKR method, the procedures developed by Chaudhury and Whitesides [27] were followed. Briefly, the radii of contact areas for 8–10 different compression loads were measured, and the contact radius versus load was plotted to extrapolate the modulus of the system from the slope of the plot. With the known modulus of the lens and assuming the materials were perfect elastic, the modulus of the coating was deduced from the modulus of the system.

The miscibility of BA and NaB with the silicone matrix was described through the analysis of the aggregate size of the antifouling compounds in the matrix. One advantage of Sylgard® 184, compared to RTV11, is that it is highly transparent so any material entrapped could be observed easily by optical microscope. Therefore, optical microscopic images were taken for the bulk of Sylgard® 184 containing the incorporated compounds. The aggregate size was analyzed by Scion Image Software.

2.4. Leaching evaluation of BA and NaB from silicones

A large sheet (total mass: 6.0 g; size: ∼0.09 cm × 64 cm^2) of silicones with 1 wt.% BA or NaB bulk entrapped was immersed in a large glass beaker containing 300 ml de-ionized (DI) water to study the leaching rate of BA and NaB into water. The conductivity of the solution at different time intervals was measured and its corresponding concentration was extrapolated via a standard calibration curve.

2.5. Bacterial attachment study

The antifouling performance of the NaB incorporated coatings would be better assessed by using the common fouling organisms, such as algae, tubeworms and diatoms. However, we had no access to such a facility during the time the study was conducted. Nevertheless, it has been indicated that bacterial attachment and subsequent biofilm formation, in general, facilitate and enhance the attachment of macro fouling organisms [28–33]. Therefore, bacterial attachment in fresh water containing enriched bacteria isolated from *Lake Erie* was conducted as a starting point to assess the coating's antifouling performance. NaB-treated and untreated silicone films coated on glass slides were placed in 60 ml amber bottles, each containing 30–40 ml of the water having the isolated bacteria. The population of bacteria in each bottle was controlled to be around 10^{11} cu/l. Care was taken to ensure all the coatings were arranged facing the bottom of the bottle to avoid the settlement of foreign species and organic matter. Coatings were observed at periodic intervals up to 1 month. At each time interval, a coating was removed, dipped

gently in fresh de-ionized water several times to remove loosely attached objects, and after drying to remove the DI water, they were immediately subjected to optical microscope observation (Transmitted light and reflected light modes for Sylgard® 184 and RTV11 systems, respectively).

3. Results and discussion

The toxicity of BA and NaB is three to five orders of magnitude lower than TBT compounds for various bacteria. Instead of killing off the bacteria, BA and NaB molecules freely floating in water were demonstrated to exhibit the true repellent mechanism and the chemical anti-adhesive mechanism against fouling organisms [14,18]. These molecules, when attached to microorganisms, could disrupt the cell's ability to maintain its suitable pH level, thus subsequent metabolism process [17]. Based on these findings, the BA and NaB molecules incorporated into the bulk of a coating should leach out in order for them to antifoul. Many factors could contribute to the leaching of the antifouling compounds from the coating carrier. Three of them investigated in this study were the properties of the carrier, the properties of antifouling compound, and the preparation methods. Before performing the leaching studies, the curing status of the coatings should be examined; an incompletely cured coating could mislead to the leaching behaviors and complicate the analysis. Variation in coating properties could be a good measure of curing status, and they will be presented first.

3.1. Coating properties variation of BA and NaB-incorporated silicones

The BA and NaB-blended coatings were cured under the same conditions as those of pure silicone coatings, the wettability and bulk properties of BA and NaB-blended silicone coatings were measured on the coatings to confirm if they were completely cured. The concentrations of BA and NaB in the silicone coatings were varied from 0 to 2 wt.%, with the water contact angle results shown in Fig. 1a. The static contact angles for control samples of Sylgard® 184 and RTV11 coatings were 106° and 100°, respectively. While the respective advancing and receding contact angles for control samples of Sylgard® 184 were 110° and 80°, they were 103° and 94° for control RTV11 samples. As shown in Fig. 1a, the contact angles essentially maintained around those values after incorporating either BA or NaB up to 2 wt.%, suggesting that most BA or NaB molecules were entrapped inside the bulk of the polymer matrix rather than aggregating on the surface. Otherwise, the contact angle would be expected to decrease due to the fact that BA or NaB has a higher surface energy than silicones, and the contact angle hysteresis (difference between the advancing and receding angles) should increase due to the in-homogeneity of aggregates present on the surface. The indifferent contact angle values of BA and NaB-blended coatings as those of pure silicone is the first indication that the NaB or BA-blended silicone coatings could be cured.

The elastic modulus of a coating is a good measure of its bulk properties. Thus, Sylgard® 184 and RTV11 coatings containing

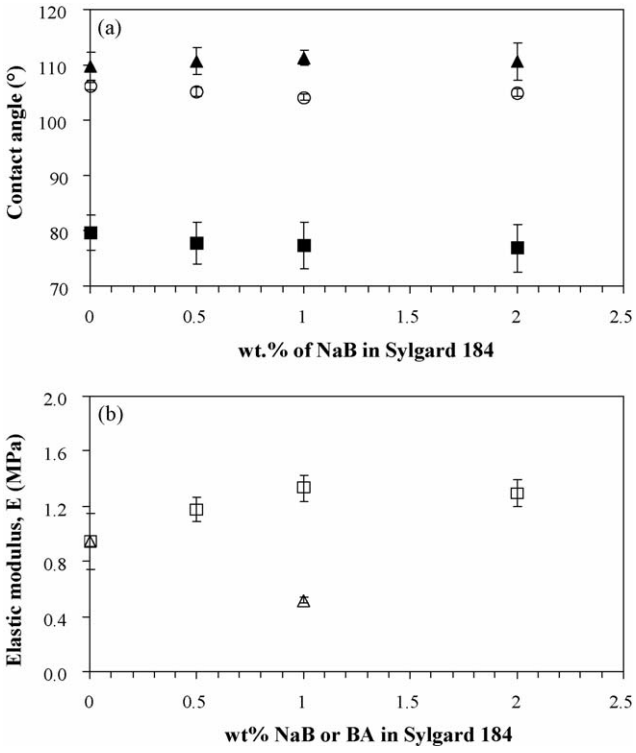

Fig. 1. (a) Water contact angles (advancing (▲), receding (■), and static (◯)) of NaB-entrapped Sylgard® 184 films and (b) bulk modulus of BA (△) and NaB (□)-entrapped Sylgard® 184 films containing various amounts of BA or NaB are presented. The vertical lines are error bars for each data point, and each data point reported was the average value of 12 and 6 measurements for contact angles and modulus, respectively.

various amounts of BA and NaB (up to 2 wt.%) were subjected to elastic modulus measurements. For control Sylgard® 184 films, both a stress–strain and the JKR techniques gave very close values in the range of 0.96–1.0 MPa, the typical elastic modulus for hydrosilylation-cured Sylgard® 184 [34]. The elastic modulus for control RTV11 was 1.56 MPa, which was also consistent with previously reported data [35]. The higher modulus of RTV11 as compared to that of Sylgard® 184 is due to the fact that RTV11 has a high content of reinforced fillers (32 wt.% $CaCO_3$). After incorporating NaB up to 2 wt.%, it was observed that the elastic moduli of both types of silicones increased slightly from those of controls. Whereas, the modulus of 1 wt.% BA/Sylgard® 184 matrix was slightly lower than the value of the control. This slight variation of the modulus could be attributed to the final distribution and aggregate size of the compound inside the bulk of the matrix. As to be seen in the next section, NaB has a uniform distribution with small aggregate size about 3 μm. Consequently, NaB could behave here as a fine reinforced filler that resulted in increasing the bulk modulus. On the other hand, BA has an irregular distribution of large crystals (to be discussed in detail later) inside the coatings, which could result in irregularity and void spaces in the matrix and hence a decrease in the bulk modulus. Nevertheless, the modulus measurements also confirmed that BA or NaB (up to 2 wt.%) has no side effects on the curing behaviors of silicones, as the bulk modulus was expected to drop substantially for an uncured coating. To summarize, the incor-

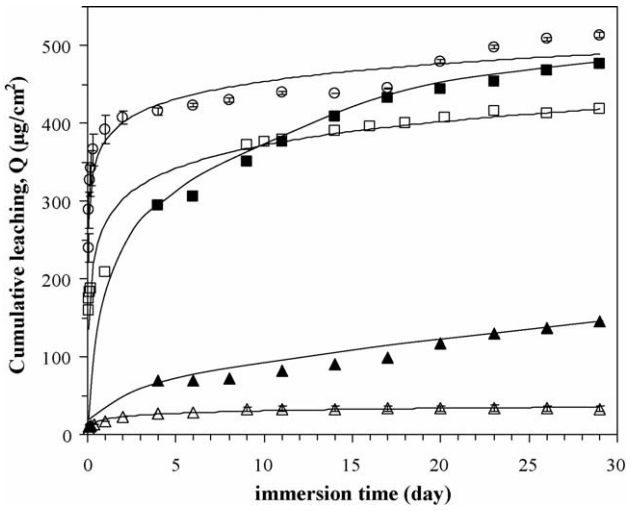

Fig. 2. Cumulative leaching amounts of BA and NaB from their incorporated coatings are summarized. The data includes the leaching of BA from BA/Sylgard® 184 with acetone (□) or toluene (◯) as the incorporating solvent, BA from BA/RTV11 (■) with acetone the incorporating solvent, and NaB from NaB/Sylgard® 184 (△) and NaB/RTV11 (▲). The common solvent used for NaB/silicones is 50/50 by weight of water/acetone. The initial concentration of the antifoulant in all coatings was ∼1 wt.%, and the solvent/polymer ratio was 20/80 by weight. The smooth lines are used to show the trends. Error for each data point (average over 2 batches) is presented by the vertical line.

poration of BA and NaB into silicone coatings (up to 2 wt.%) did not considerably affect either the surface or bulk properties of the coatings, suggesting a complete curing of the coatings and the probable retention of the foul-release property of both types of silicones.

3.2. Leaching rates of BA and NaB from silicones into water

As shown in Fig. 2, for any particular coating (1 wt.% BA or NaB in silicone) the entrapped compound leached out fast in the initial few days and continued to leach with a much slower steady state pace until the content either completely exhausted or up to the 4 months we monitored. As compared to NaB, much higher leaching was observed for BA regardless of the matrix (Sylgard® 184 or RTV11) or the solvent (acetone or toluene) used. For BA/Sylgard® 184 coatings, prepared using acetone as the solvent, after 1 week and 1 month of immersion, about 73 and 85% of the initial BA content, respectively, had leached out from the coating. When toluene was used as the solvent or RTV11 as the carrier (acetone as the solvent), BA completely depleted from the coating in about 1 month. For NaB/Sylgard® 184 coatings, the slowest leaching was observed, with the leached percentages to its initial mass of 6.7, 7.3, and 9.8%, respectively, after 1 week, 1 month, and 4 months being in water. Changing the coating carrier to RTV11 did considerably affect the leaching. For 1 wt.% NaB/RTV11 after 1 week, 1 month, and 4 months of immersion, it was found that about 16, 31, and 88% of the initial mass, respectively, had leached out. For both BA and NaB, when RTV11 was used as the coating carrier, the steady state leaching rate of coatings prepared under the same conditions was at least three times faster than that with Sylgard® 184 as the carrier.

Three reasons can be attributed to the higher leaching of NaB from RTV11 compared to that of Sylgard® 184. First, partial degradation and erosion of the RTV11 matrix in water, which has been confirmed experimentally by Bullock et al. [36], could be contributing and facilitating the leaching. Second, RTV11 has a high content of inorganic fillers including $CaCO_3$ (32 wt.%), which has a pore volume of 0.1–0.8 cm^3/g [37,38]. At this high filler content, filler agglomeration, which is a result of incomplete dispersion or flocculation, is highly possible, which could lead to "voids" in-between the filler particles and at the filler/polymer interface [39] allowing water molecules to seep into the silicone matrix through these empty spaces and carry the dissolved NaB molecules with them as they leave the coating. Third, the reported solubility of water in PDMS is 7000 and 700 ppm for filled and unfilled silicone, respectively, and the reported water diffusivity in silicone is 8.6×10^{-7} cm^2/s at 25 °C [40]. Consequently, water permeability, which is a product of its solubility and diffusivity in the matrix, will be higher in the filled silicone matrix compared to the unfilled one.

Apart from the specific properties of the coating carrier, many other factors could contribute to the leaching of the antifouling compounds from the coating carrier. In this study, we noticed that the morphological structures and the distribution of the antifouling compound appeared to play important roles in leaching when carriers were immiscible with the antifoulant compounds.

3.3. Distribution and morphological structures of BA and NaB in silicone

It is believed that the miscibility of BA or NaB with the silicone matrix plays an important role for the distribution of the compound within the silicone coatings. Both BA and NaB were immiscible with highly non-polar silicone. Even when the compound was mixed into the silicone coatings using a common solvent, the compound phase separated from silicone upon removal of the solvent. Images in Figs. 3 and 4 showed very distinguishable different morphological structures of BA and NaB inside the Sylgard® 184 matrix. For BA, large (hundreds of microns) crystals were observed to disperse randomly inside the carrier, whereas for NaB, small (a few microns or tens of microns) aggregates were distributed uniformly throughout the carrier. The number density of the BA crystals (1–2 mm^{-2} and 7–8 mm^{-2} using toluene and acetone, respectively) were much lower than that of the NaB aggregates. It is possible that occasionally, some large crystals could span the entire thickness (∼500–800 μm) of the coating, thus providing easy access for water to reach and dissolve the BA and then carry it out of the coating.

For BA and NaB-incorporated Sylgard® 184 coatings, the preparation conditions were systematically varied to examine their effects on the distribution and morphological structures of BA and NaB inside the coating matrix. For BA/Sylgard® 184 systems, the coatings were prepared using four different organic solvents (toluene, acetone, acetonitrile, and di-ethyl ether), following the procedures described previously in Section 2. As shown in Fig. 3, large crystals were observed inside the polymer matrix for all types of solvents used. Toluene was found

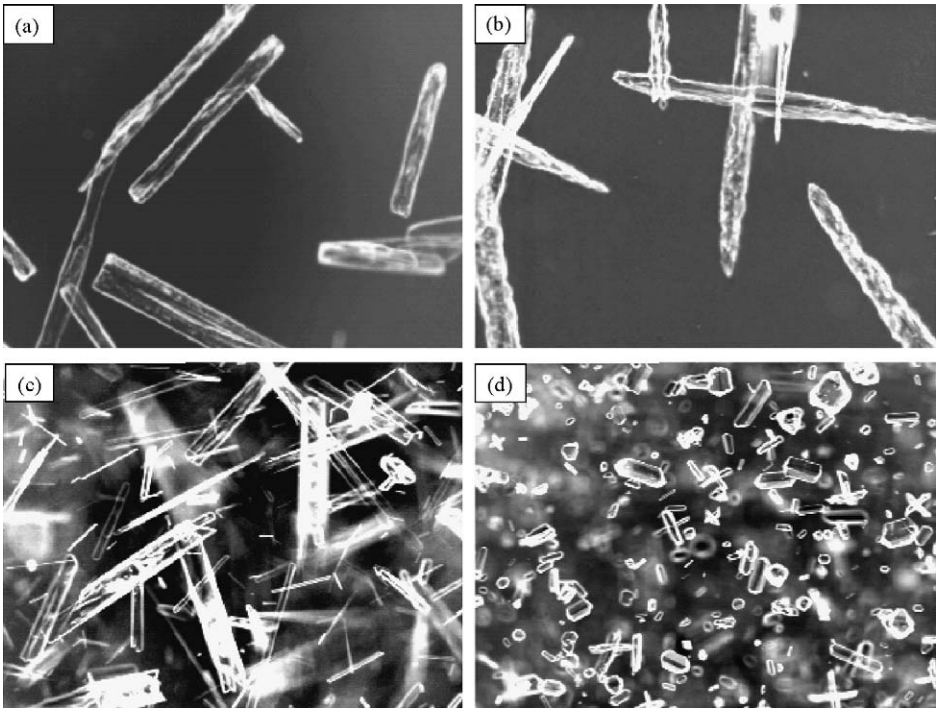

Fig. 3. Optical microscope (bright field) images of the resulting BA distribution in the bulk of Sylgard® 184 matrix when (a) toluene, (b) acetone, (c) acetonitrile, or (d) ether was used as the common solvent to mix BA with Sylgard® 184. The image size is 2850 μm × 2400 μm for (a), and 1140 μm × 960 μm for (b–d). To show the crystals more clearly, the "negative" of the bright field image was presented here.

to result in the largest crystals (∼600–1000 μm), and di-ethyl ether produced the smallest ones (50–100 μm), whereas acetone and acetonitrile resulted in crystals somewhere in between (∼200–500 μm). The estimated size here refers to the average length (the largest dimension) of the crystal. From Fig. 3, it is also clear that ether resulted in a more uniform distribution of the smallest crystals (the number density was 90–95 mm^{-2}) compared to the other solvents. The effect of solvent on bulk distribution of BA in the coating could be understood by considering four factors: the chemical nature of the solvent, its boiling point (or alternatively the volatility), BA solubility in the solvent, and solvent-matrix miscibility. The four solvents selected here are representative of different chemical classes: toluene (an aromatic), acetone (a ketone), acetonitrile (a nitrile), and di-ethyl ether (an ether). The physical properties relating to the miscibility of these solvents with both BA and silicones are summarized in Table 1. The experimentally measured solubility of BA in toluene, acetone, acetonitrile, and ether was around 10, 32, 14, and 33 wt.%, respectively [41]. The normal boiling point of toluene, acetone, acetonitrile, and ether are 111, 56, 82, and 35 °C, respectively. By considering the differences in solubility parameters of silicone and the solvent, $\Delta\delta$, the high BA solubility in ether, and the low boiling point of ether, it was not surprising that the smallest crystals resulted when ether ($\Delta\delta = 0.2\ MPa^{1/2}$) was used as the solvent. With toluene, a high value of $\Delta\delta$ ($3.3\ MPa^{1/2}$) and the highest boiling point but the lowest BA solubility, as the solvent, the largest crystals were formed. The crystal formation capability of BA, as illustrated using various solvents could likely be the primary reason for its fast leaching and relatively short period of antifouling effectiveness reported in the literature [14], even though in that study a vinyl-rosin coating was used.

For NaB/Sylgard® 184 systems, the preparation conditions were systematically varied to investigate their effects on the morphological structures and later the leaching. The parameters varied were: solvent composition (acetone/water ratio), solvent/polymer ratio, and final concentration of NaB in the matrix. We chose the base case conditions to be: 50/50 water/acetone ratio, 20/80 solvent/polymer ratio, and 1 wt.% NaB in the matrix, with all ratios in mass basis. When varying any one parameter, the other parameters were fixed at the base case conditions. As shown in Figs. 4 and 5, the bulk aggregate size was minima around the value of 3 μm in the range of 20–50% water content, increased to about 8 μm at 80% water content, and then increased very sharply after that ratio. Increasing the wt.% NaB/polymer from 1 to 2 wt.% caused the aggregate size to increase to about 5 μm, whereas it stayed around 3 μm when the wt.% NaB/polymer was reduced from 1 to 0.5 wt.%. The solvent/polymer ratio of 20/80 is the optimum ratio that resulted in minimum aggregate size (3 μm), whereas increasing the solvent/polymer ratio from 30/70 or decreasing it to 10/90 has resulted in increasing aggregate size considerably to about 42 and 14 μm, respectively. As a control experiment, the above miscibility experiments were repeated for the same sets of conditions, except that all mixtures are prepared without heating. The mixtures were kept inside the air hood for 4 days to dry off the solvent at room temperature, and then optical microscope imaging was taken for the bulk phase before adding the catalysts. The objective here is to examine the thermodynamics phase separation of the solvent/polymer mixture with minimal distur-

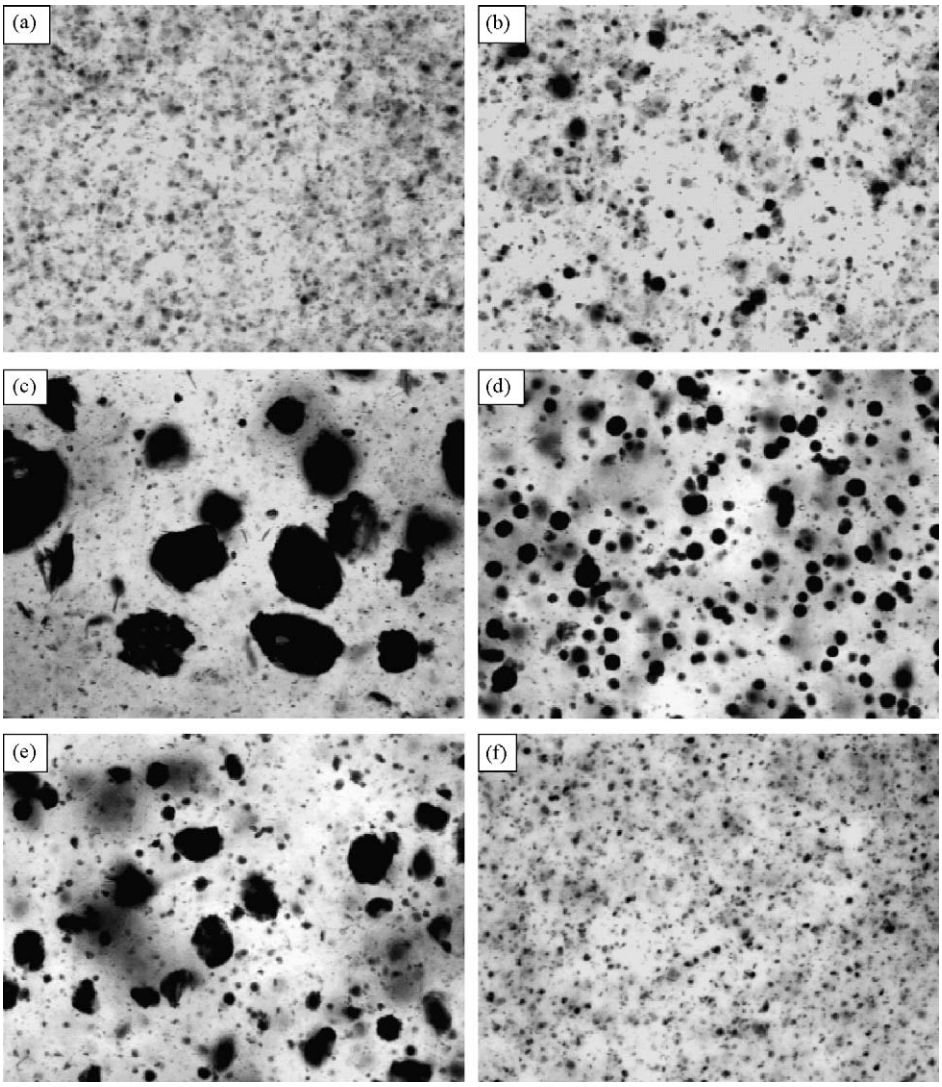

Fig. 4. Optical microscope (bright field) images (570 μm × 480 μm) of 1 wt.% NaB distributed in Sylgard® 184 matrix, (a) the base case conditions: 50/50 water/acetone, 20/80 solvent/polymer; (b) 80/20 water/acetone, 20/80 solvent/polymer; (c) 90/10 water/acetone, 20/80 solvent/polymer; (d) 50/50 water/acetone, 10/90 solvent/polymer and (e) 50/50 water/acetone, 30/70 solvent/polymer. The morphology of the coating contains 0.5% NaB prepared under base case condition is shown in (f). All the values are based on weight.

Table 1
Relevant physical parameters of different materials used in this study are summarized

Material	V (cm^3/mol)	δ $(J/cm^3)^{1/2}$	$\Delta\delta_{12}$ $(J/cm^3)^{1/2}$	χ_{12}	Boiling point (°C)
Water	18.2	47.9[a]	33.0	8.000	100
Acetone	74.0	20.3[a]	5.4	0.871	56
Acetonitrile	52.6	24.6[a]	9.7	1.998	81.5
Toluene	106.8	18.2[a]	3.3	0.469	110.6
Ether	105	15.1[a]	0.2	0.002	34.6
BA	92.5	22.9[b]	8.0	2.389	–
NaB	100.1	35.8[b]	20.9	17.648	–
PDMS	5714[c]	14.9[a]	–	–	–

V and δ are the molar volume and the solubility parameter of the material, respectively. $\Delta\delta_{12}$ and χ_{12} are, respectively, the difference in solubility parameters and the interaction parameter between the material and silicone (i.e. PDMS).

[a] Value obtained from reference [43].
[b] Value obtained from reference [44].
[c] Value obtained from reference [45].

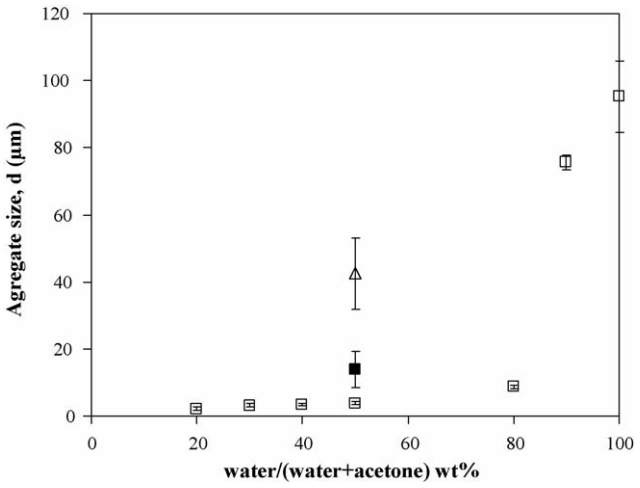

Fig. 5. Average aggregate size (*d*: diameter) of 1 wt.% of NaB inside the bulk of Sylgard® 184 matrix is plotted against the wt.% of water in the mixed-solvent of water/acetone used for incorporation. The initial solvent and polymer ratios used were 20/80 (□), 10/90 (■), and 30/70 (△). Error for each data point (average over 24 measurements) is presented by the vertical line.

bance. The same results were observed: the set of conditions that resulted in minimal aggregate size were 20/80 solvent/polymer, and 20/80–50/50 water/acetone, where the aggregate size at these conditions was measured to be around 5 μm.

The miscibility of a substance (1) with a polymer (2) can be roughly predicted by the substance-polymer interaction parameter, χ_{12}. According to the "Flory–Huggins" theory, χ_{12} is given by [42]:

$$\chi_{12} = \frac{V_1}{RT}(\delta_1 - \delta_2)^2 \quad (1)$$

where V_1 is the molar volume of the smaller species, the substance in our case, R and T, respectively, the ideal gas constant and the temperature, and δ_1 and δ_2 are respectively the solubility parameters of the substance and the polymer. A smaller χ_{12} indicates a higher chance that the system would be miscible, and a value of $\chi_{12} < 0.5$ is the Flory–Huggins criterion for a solvent/polymer system to be completely miscible. Table 1 summarizes the χ_{12} values of various substances and silicone (i.e. PDMS). First, the χ_{12} values for BA/PDMS and NaB/PDMS are 2.389 and 17.648, indicating that both compounds are likely not miscible with PDMS, as observed experimentally. For the four solvents used in BA/PDMS systems, it is clear that ether is most miscible with PDMS ($\chi_{12} = 0.002$), thus the domains of ether + BA would likely be the smallest as ether being completely evaporated and resulting in the smallest BA crystals as compared to other solvents. For NaB/PDMS systems, water is highly immiscible with PDMS ($\chi_{12} = 8.000$) while acetone has some miscibility with PDMS, hence the size of NaB aggregates increased as the water content (in the mixed solvent of water/acetone) increased. In a more general form, χ_{12} can be qualitatively described as:

$$\chi_{12} = \chi_{12,d} + \chi_{12,fv} + \chi_{12,sp} \quad (2)$$

where $\chi_{12,d}$ accounts for the dispersion interactions, $\chi_{12,fv}$ accounts for the interactions resulting from the free volume effect, and $\chi_{12,sp}$ accounts for the specific interactions such as acid–base interactions or H-bonding. However, the "Flory–Huggins" theory only considers the dispersion interactions and totally neglects the other two types of interactions, which might result in errors in estimating the values of χ_{12} presented in Table 1. For example, neglecting the free volume effect is based upon the assumption that no volume changes upon mixing, which is rarely satisfied for mixing large macromolecules with solvents or additives of much smaller size, such as BA or NaB. Specific interactions, including self-interactions, could exist in our systems, and decrease the miscibility of the BA or NaB with silicone. Nevertheless, the rough prediction based on the "Flory–Huggins" interaction parameter did qualitatively describe our systems.

3.4. Relationship between NaB aggregate size and its leaching rates from silicones

The cumulative leaching (Q) of NaB for NaB/Sylgard® 184 samples prepared using the mixed solvent of water/acetone under different water/acetone ratios, different solvent/polymer ratios, and different wt.% NaB in the matrix is summarized in Fig. 6. The general trend, regardless of preparation conditions, was observed. NaB leached out in two stages, a first fast stage occurred in the initial few days, followed by a second steady stage having a much slower rate. The Q value is higher with a larger initial aggregate size.

To relate the leaching and NaB aggregate size, one may assume that the blending of NaB with the coating using a com-

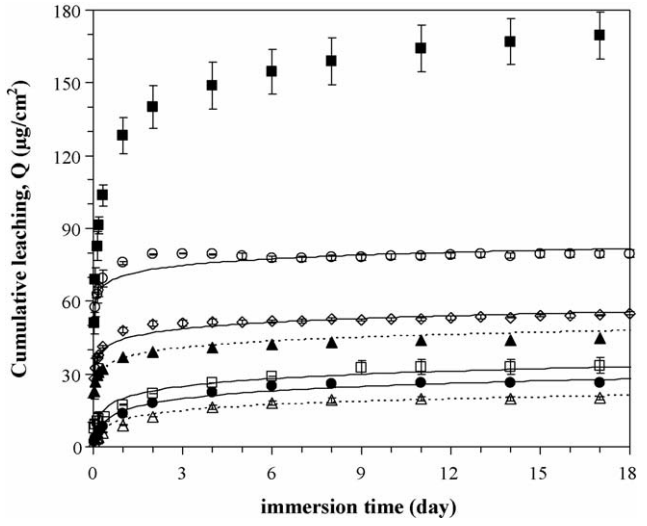

Fig. 6. Cumulative leaching (Q) of NaB from Sylgard® 184 coatings prepared under different conditions is presented. (△) and (▲) represent 0.5 wt.% NaB/polymer prepared using 20/80 solvent/polymer and 10/90 solvent/polymer, respective, and the solvent is 50/50 water/acetone; (●), (□), (◊), and (◯) symbolize 1 wt.% NaB/polymer prepared with 20/80 water/acetone and 20/80 solvent/polymer, 50/50 water/acetone and 20/80 solvent/polymer, 50/50 water/acetone and 10/90 solvent/polymer, and 50/50 water/acetone and 30/70 solvent/polymer, respectively. (■) denotes 2 wt.% NaB/polymer prepared using 50/50 water/acetone and 20/80 solvent/polymer. The smooth lines are used to show the trends. Error for each data point (average over 2 batches) is presented by the vertical line, and all the values are based on weight.

mon solvent resulted in a uniform distribution of NaB aggregates, presumably with the same size, throughout the entire volume of the coating. The number of aggregates per unit volume of the coating is given the symbol of n. The coating could be uniformly divided into a series of thin sub-layers each with a thickness of h_j and the number of NaB aggregates of n_j ($n_j/n = h_j/h$). By assuming that the aggregates are spherical, n can be estimated as:

$$n = \left[\frac{\omega_{AF}/\rho_{AF}}{1/\rho_c}\right]\frac{6}{\pi d^3} \quad (3)$$

where ω_{AF} is the initial weight or mass fraction of the antifoulant in the coating, ρ_{AF} and ρ_c the density of antifoulant (i.e. NaB) and the coating, respectively, and d is the initial diameter of the antifoulant aggregate (measured experimentally). Eq. (3) explicitly includes the initial concentration of NaB in the matrix and the size of NaB aggregates.

As a rough approximation, the sub-layer thickness h_j is set to $\sim\alpha d$, where the factor α (>1) is used to account for the spacing in-between the aggregates, with h (~900 μm) known and d measured experimentally, the mass ratio n_j/n can be estimated. As n increases, the distribution becomes more uniform with smaller aggregates, resulting in a small mass fraction of NaB in the top (i.e. first) layer relative to that in the entire volume. Once immersed in water, most of NaB aggregates present in the top layer (n_j) were assumed to dissolve and leach out within a short period of time, and contributed to the first fast leaching stage. Having a larger number of small aggregates will result in a lower initial leaching of the compound, thus minimizing the unavoidable waste occurring during the fast leaching period. If these assumptions were correct, the fractional cumulative leaching (Q/Q_0, with Q_0 being the initial mass of NaB in the coating per unit area) during the first fast leaching stage should be equivalent to the fractional mass present in the first layer to the total NaB mass in the coating (n_j/n). Fig. 7a presents the first fast stage leaching of NaB versus number of aggregates presented in the NaB/Sylgard® 184 coatings prepared under different conditions; while the insert in Fig. 7a summarizes the relationship between the first fast leaching values and the aggregates presented in the top layer of the coating. As can be seen in the insert, an excellent linear fit ($R^2 = 0.98$) was obtained, with the slope (1.06) almost equal to unity, indicating that the above approximations are valid. Therefore, regardless of the preparation conditions, NaB that existed in the first layer always leached out rapidly as compared to the rest within the subsequent layers. In order to minimize the unnecessary loss of antifoulant during the first fast leaching, it is more desired to have a smaller value of n_j/n, which can be obtained by generating more aggregates of smaller sizes.

The leaching mechanism of an antifoulant from a polymer matrix depends largely on its solubility in the matrix. If it has a high solubility (e.g. >1 wt.%), the leaching primarily follows a diffusion–dissolution mechanism, which takes place in the continuum of the polymer phase. If the solubility is very low (e.g. <0.1 wt.%), the mechanism is controlled by the channeling/pores formation, where the pores and channels are formed progressively due to water diffusion within the aggregate phase and/or at the polymer/aggregate interface. If the solubility is intermediate, both mechanisms would contribute to the leaching. Since the solubility of NaB in silicones was very low, most likely its leaching from silicone coatings is governed by the second mechanism. The slow processes of water diffusion and penetrating into the coating to dissolve NaB aggregates and then transporting the freshly formed NaB/water solution out of the coating would be the primary factor for the second slow steady state of leaching. As NaB aggregates are being dissolved, channels/pores are being formed, which could then affect and complicate the leaching process. Therefore, different from the fast initial leaching, it may not be possible to establish a direct relationship between the leaching rate of the slow stage and the initial aggregate size or the (n_j/n) ratio (Fig. 7b). Nevertheless, a faster leaching for a coating containing larger aggregates of the incorporated compound was clearly observed. The mechanisms of the slow leaching stage will need further investigations.

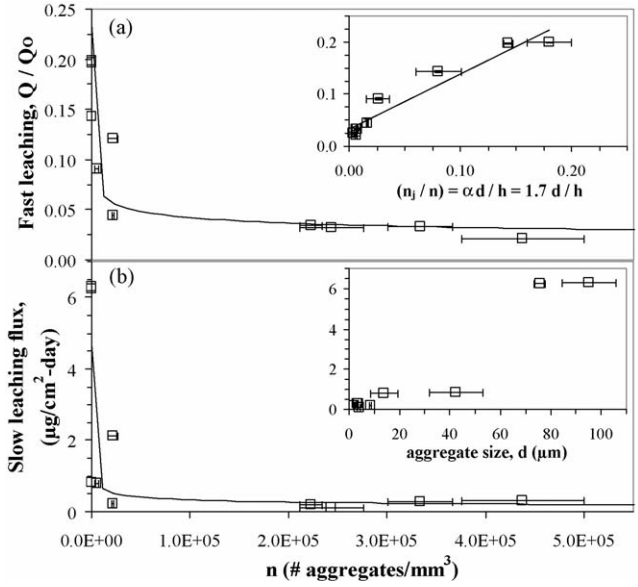

Fig. 7. (a) The fractional cumulative amount (Q/Q_0) leached out of NaB form Sylgard® 184 coatings, prepared under different conditions, during the first fast leaching stage is summarized. Q_0 is the initial unit area mass of NaB in the coating, and the Q values are the experimentally measured amounts of NaB leached out after 1 day of immersion, where each Q value is an average of two batches. When plotted against the ratio of the NaB mass presented in the first layer of the coating to the total mass in the entire coating (insert of (a), n_j/n, where n_j and n are the initial number of aggregates exist in the first layer and the entire coating, respectively) and with a proper value of α ($\alpha = 1.7$) a straight line with a slope equals to unity was obtained. In (b) the average leaching flux from day 6 to 18, obtained from the slope of the straight line of Q vs. time, was plotted against the number of aggregates (or aggregate size, the insert), and no simple relationship was found.

3.5. Bacterial attachment study of NaB-treated silicone

To evaluate antibacterial behaviors of the coatings, bacterial attachment studies using fresh water containing indigenous enriched microbial consortium isolated from *Lake Erie* water were performed. 1 wt.% NaB containing silicone coatings and pure silicone coatings were submerged in the above water at periodic intervals up to 1 month. The reason we only performed

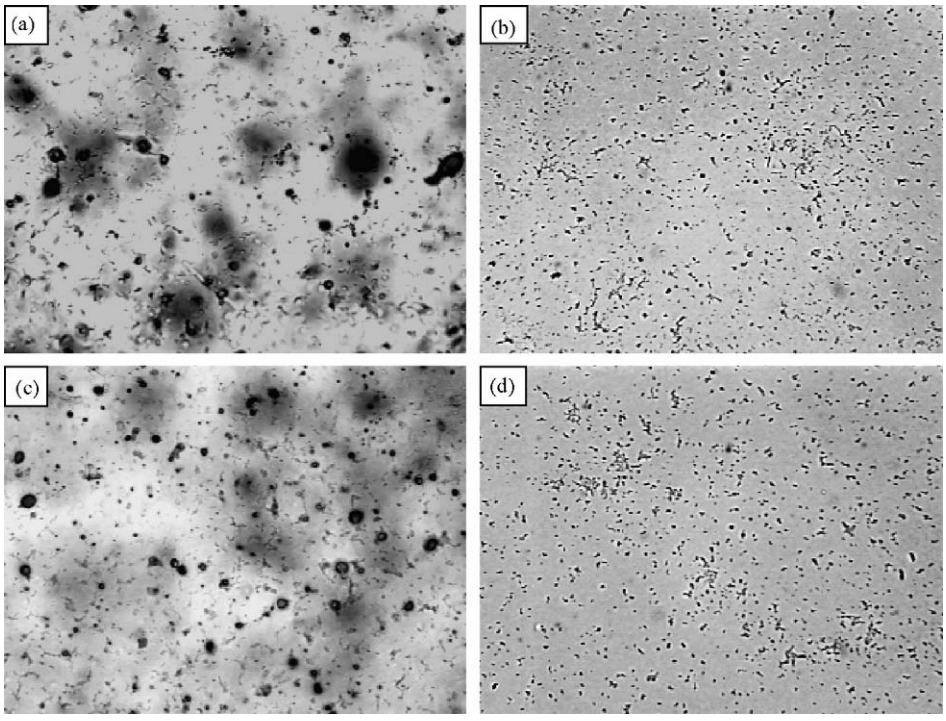

Fig. 8. Optical microscope images (285 μm × 215 μm) of bacterial attachment on 1 wt.% NaB-blended Sylgard® 184 (a and c) and control Sylgard® 184 (b and d) after the coatings have been immersed in water containing *Lake Erie* bacteria for 2 weeks (a and b) and 4 weeks (c and d).

bacterial attachment on NaB incorporated silicone coatings was due to the fact that BA leached out too fast from its incorporated coating. For real applications, BA incorporated coatings will unlikely be used. Some representative biofilm morphologies are shown in Fig. 8. For a particular period of immersion, an average of 45–50% reduction in bacterial coverage was achieved for 1 wt.% NaB/Sylgard® 184 coatings as compared to Sylgard® 184 alone. By comparing control samples of RTV11 and Sylgard® 184, it was observed that RTV11 had a higher tendency for biofilm formation than that of Sylgard® 184. This is attributed to the fact that RTV11 has a slightly higher surface energy, bulk modulus, and surface roughness than those of Sylgard® 184. For NaB-containing RTV11, the morphology was hard to be observed and the bacteria were difficult to be identified from the pictures directly. To differentiate the bacteria from other objects, the RTV11 coating surfaces were physically cleaned by Scotch® tape, and pictures were taken before and after cleaning. For control RTV11 coatings, the surface became very clean after applying the tape, indicating that the removed objects were likely bacterial biofilm. For NaB–RTV11 coatings, however, the morphology did not changed much after applying the tape, suggesting that the irregularities seen were parts of the coatings surface and were not bacterial biofilm. The irregularities seen in/on NaB–RTV11 coatings were mostly holes (verified by atomic force microscopic scanning) likely generated by NaB leaching, and the reason that they are much larger than the holes seen in/on NaB–Sylgard® 184 coatings is the much faster leaching of NaB from RTV11 than from Sylgard® 184. To summarize, a clear reduction in bacterial attachment on the NaB-treated coatings was observed, which suggests that NaB can be effective in inhibiting bacterial attachment when entrapped into a coating.

4. Conclusions

Benzoic acid (BA) and sodium benzoate (NaB), both low toxicity compounds, were successfully incorporated into Sylgard® 184 and RTV11 silicone coatings. Minimal effect on the bulk and surface properties of the coatings was observed when the concentration of the compound varied from 0 to 2 wt.%. BA was shown to form large crystals in the bulk of the matrix upon evaporation of the solvent. The formation of large crystals could be the main reason for the fast leaching of BA from coating carriers, thus truncating its usage as an antifoulant to be incorporated into a coating. NaB, on the other hand, exhibited slow and controllable leaching by varying the preparation conditions, which may have significant effects on its morphological structures and final distribution in the matrix, hence the leaching. Although the toxicity of NaB is four to five orders of magnitudes lower than commonly used antifoulants such as TBT and SeaNine 211, NaB incorporated coatings exhibited enhanced antibacterial behaviors as compared to silicone coatings alone. The promising antibacterial attachment results of NaB-incorporated coatings coupled with the simplicity of varying the preparation conditions to achieve the desired leaching suggest that NaB could be an environmentally friendlier alternative to the currently used toxic biocides in antifouling applications.

Acknowledgments

Financial support from Ohio Board of Regents (R5905-OBR) and Ohio Sea Grant (Project: R/MB-2) is greatly appreciated. We are grateful to Dr. T. Cutright and Mr. Q. Xu for assisting the bacterial attachment studies. Mr. Al-Juhni is also very gratified

to the Ministry of Higher Education, Saudi Arabia, for providing him a full scholarship throughout his entire Ph.D. study.

References

[1] L.V. Evans, N. Clarkson, Antifouling strategies in the marine environment, J. Appl. Bacteriol. Symp. Suppl. 74 (1993) 119S–129S.

[2] A. Davis, P. Williamson, Marine Biofouling: A Sticky Problem, NERC News, 1995.

[3] P.K. Abdul Azis, I. Al-Tisan, N. Sasikumar, Biofouling potential and environmental factors of seawater at a desalination plant intake, Desalination 135 (2001) 69–82.

[4] A.U. Malik, T.L. Prakash, I. Andijani, Failure evaluation in desalination plants - Some case studies, Desalination 105 (1996) 283–295.

[5] L.F. Melo, T.R. Bott, Biofouling in water systems, Exp. Thermal. Fluid Sci. 14 (1997) 375–381.

[6] T.S. Wood, T.G. Marsh, Biofouling of wastewater treatment plants by the freshwater bryozoan, Plumatella vaihiriae, Water Res. 33 (1999) 609–614.

[7] M. Al-Ahmed, F.A. Abdul-Aleem, A. Mutairi, A. Ubaisy, Biofouling in RO membrane systems. Part 1: Fundamentals and control, Desalination 132 (2000) 173–179.

[8] V. Axiak, A.J. Vella, D. Agius, P. Bonnici, G. Cassar, R. Cassone, P. Chircop, D. Micallef, B. Mintoff, M. Sammut, Evaluation of environmental levels and biological impact of TBT in Malta (central Mediterranean), Sci. Total Environ. 258 (2000) 89–97.

[9] E. Haslbeck, C.J. Kavanagh, H.W. Shin, W.C. Banta, P. Song, G.I. Loeb, Minimum effective release rate of antifoulants: measurement of the effect of TBT and zosteric acid on hard fouling, Biofouling 10 (1996) 175–186.

[10] M. Champ, A review of organotin regulatory strategies, pending actions, related costs and benefits, Sci. Total Environ. 258 (2000) 21–71.

[11] S.K. Sagoo, R. Board, S. Roller, Chitosan potentiates the antimicrobial action of sodium benzoate on spoilage yeasts, Lett. Appl. Microbiol. 34 (3) (2002) 168–172.

[12] H. Haque, T.J. Cutright, B.-m.Z. Newby, Effectiveness of sodium benzoate and benzoic acid as freshwater low toxicity antifoulants when dispersed in solution and entrapped in silicone coatings, Biofouling 21 (2005) 109–119.

[13] D. Sundberg, N. Vasishtha, R.C. Zimmerman, C.M. Smith, Selection, design and delivery of environmentally benign antifouling agents, Nav. Res. Rev. XLIX (1997) 51–59.

[14] A. Railkin, Marine Biofouling: Colonization Processes and Defenses, CRC Press, Boca Raton, 2004, pp. 194–225.

[15] E. Lueck, Benzoic Acid, in: Antimicrobial Food Additives. Characteristics, Uses, Effects, Springer-Verlag, Berlin, 1980, pp. 210–217.

[16] J.S. Chapman, Biocide resistance mechanisms, Int. Biodet. Biodeg. 51 (2003) 133–138.

[17] T. Eklund, The effect of sorbic acid and esters of *p*-hydroxybenzoic acid on the proton motive force in Escherichia coli membrane vesicles, J. Gen. Microbiol. 131 (1985) 73–76.

[18] V. Vetere, M. Perez, M. Garcia, M. Deya, M. Stupak, B. del Amo, A non-toxic antifouling compound for marine paints, Surf. Coat. Int. 12 (1999) 586–589.

[19] M.E. Stupak, M.T. Garcia, M.C. Perez, Non-toxic alternative compounds for marine antifouling paints, Int. Biodet. Biodeg. 52 (2003) 49–52.

[20] R.F. Brady, Clean hulls without poisons: devising and testing nontoxic marine coatings, J. Coat. Technol. 72 (2000) 45–56.

[21] R.F. Brady, I.L. Singer, Mechanical factors favoring release from fouling release coatings, Biofouling 15 (2000) 73–81.

[22] R.F. Brady, Properties which influence marine fouling resistance in polymers containing silicon and fluorine, Prog. Org. Coat. 35 (1999) 31–35.

[23] K.J. Wynne, G.W. Swain, R.B. Fox, S. Bullock, J. Two silicone nontoxic fouling release coatings: hydrosilation cured PDMS and $CaCO_3$ filled, ethoxysiloxane cured RTV11, Biofouling 16 (2000) 277–288.

[24] F.F. Estarlich, S.A. Lewey, T.G. Nevell, A.A. Thorpe, J. Tsibouklis, A.C. Upton, The surface properties of some silicone and fluorosilicone coating materials immersed in seawater, Biofouling 16 (2000) 263–275.

[25] B. Watermann, H.D. Berger, H. Sonnichsen, P. Willemsen, Performance and effectiveness of non-stick coatings in seawater, Biofouling 11 (1997) 101–118.

[26] K.L. Johnson, K. Kendall, A.D. Roberts, Surface energy and the contact of elastic solids, Proc. R. Soc. Lond. A324 (1971) 301–313.

[27] M.K. Chaudhury, G.M. Whitesides, Direct measurement of interfacial interactions between semispherical lenses and flat sheets of poly(dimethylsiloxane) and their chemical derivatives, Langmuir 7 (1991) 1013–1025.

[28] M.A. Miller, J.C. Rapean, W.F. Whedon, The role of slime film in the attachment of fouling organisms, Biol. Bull. 94 (1948) 143–157.

[29] A. Daniel, Factors influencing the settlement of marine foulers and borers in tropical seas, in: Proceedings of the First Summer School of Zoology, New Delhi, India, 1963, pp. 363–382.

[30] D.J. Tighe-Ford, M.J.D. Power, D.C. Vaile, Laboratory rearing of barnacle larvae for antifouling research, Helgol. Meeresuntters 20 (1970) 393–405.

[31] C.D. Todd, M.J. Keough, Larval settlement in hard substratum epifaunal assemblages: a manipulative field study of the effects of substratum filming and the presence of incumbents, J. Exp. Mar. Biol. Ecol. 181 (1994) 159–187.

[32] M.J. Keough, P.T. Raimondi, Responses of settling invertebrate larvae to bioorganic films: effects of different types of films, J. Exp. Mar. Biol. Ecol. 185 (1995) 235–253.

[33] M.J. Keough, P.T. Raimondi, Responses of settling invertebrate larvae to bioorganic films: effects of large-scale variation in films, J. Exp. Mar. Biol. Ecol. 207 (1996) 59–68.

[34] D.T. Eddington, W.C. Crone, D.J. Beebe, Development of process protocols to fine tune polydimethylsiloxane material properties, in: 7th International Conference on Miniaturized Chemical and Biochemical Analysis Systems, Squaw Valley, California, USA, October 5–9, 2003, pp. 1089–1092.

[35] J.G. Kohl, R.N. Bolstes, A study on the elastic modulus of silicone duplex or bi-layer coatings using micro-indentation, Prog. Org. Coat. 41 (2001) 135–141.

[36] S. Bullock, E.E. Johnston, T. Willson, P. Gatenholm, K.J. Wynne, Surface science of a filled polydimethylsiloxane-based alkoxysilane-cured elastomer: RTV11, J. Colloid Interface Sci. 210 (1999) 18–36.

[37] G. Wypych, Handbook of Fillers, Transcontinental Printing Inc., Toronto, 1999, p. 48.

[38] Y. Shiroki, Int. Polym. Sci. Technol. 20 (6) (1993) 12–21.

[39] G.K. van der Wel, O.C.G. Adan, Moisture in organic coatings—a review, Prog. Org. Coat. 37 (1999) 1–14.

[40] S. Banerjee, R. Asrey, C. Saxena, V. Vyas, A. Bhattacharya, Kinetics of diffusion of water and DMMP through PDMS membrane using coated quartz piezoelectronic sensor, J. Appl. Polym. Sci. 65 (1997) 1789–1794.

[41] G.L. Perlovich, B. Annette, Thermodynamics of solutions I: benzoic acid and acetylsalicylic acid as models for drug substances and the prediction of solubility, Pharm. Res. 20 (3) (2003) 471–478.

[42] P.J. Flory, Principles of Polymer Chemistry, Cornell University Press, Ithaca, 1953.

[43] F. Rodriguez, Principles of Polymer Systems, Hemisphere Publishing Corp., New York, 1989, pp. 29–31.

[44] P. Bustamante, M.A. Pena, J. Barra, The modified extended Hansen method to determine partial solubility parameters of drugs containing single hydrogen bonding group and their sodium derivatives, Int. J. Pharm. 194 (2000) 117–124.

[45] A. Galliano, S. Bistac, J. Schultz, Adhesion and friction of PDMS networks: molecular weight effects, J. Colloid Interface Sci. 265 (2003) 372–379.